

Continuous Compression Stress Relaxation of Rubber Materials: Testing and Simulation

Abraham Pannikottu, Charles Lu, Mark Centea

Akron Rubber Development Laboratory, Inc.
2887 Gilchrist Road, Akron, OH 44305

1. Introduction

Rubber is extensively used as gasket and seal materials. The force applied during clamp-up is stored in the deformed rubber and exerts back pressure against the flanges maintaining a tight seal. This sealing force will decrease with stress relaxation. It will also change with temperature variation and resultant expansion or contraction of the seal, and change as the rubber swells or shrinks in the fluid being sealed.

Stress relaxation is regarded as being the most convenient method of evaluating the suitability of a given rubber material for sealing applications (Zhang and Birley 1992, Bunting *et al.*, 1992). However, the conventional test, particularly the short-term test, can be misleading, since in actual application the rubber will function over a wide temperature range between metal flanges. The current continuous compression stress relaxation (CCSR) test aims to offer an improved method of evaluating rubber compounds.

2. ARDL Continuous Compression Stress Relaxation Test

2.1 Apparatus

The ARDL continuous compression stress relaxation (CCSR) apparatus is shown in Figure 1a and Figure 1b. The apparatus consists of 5 fixtures, sitting inside the temperature chamber. In each fixture, the specimen is placed between the base plate and compression plate. The compression is set by a high-resolution screw adjuster with a lock nut, which maintains the compression at the desired constant value. A load cell is installed in series between the screw adjuster and the plunger, and connected to a multi-functional measuring

instrument. This measuring instrument is interfaced with a microcomputer through a data acquisition card. Experimental data (force, displacement, temperature, time, etc.) are recorded continuously during a test.

The potential application of the continuous compression stress relaxation test is to examine the effect of thermal cycling on retention of sealing force of rubber components. For this, an accurate cycling heating and cooling system is required. A temperature chamber is built inside the current CCSR apparatus with a thermo-electric plate. A power supply and a thermal-electric cooling system are used to control the temperature, ranging from $-40\text{ }^{\circ}\text{C}$ to $+150\text{ }^{\circ}\text{C}$ with tolerance of $\pm 0.5\text{ }^{\circ}\text{C}$.

2.2 Experimental procedure

Prior to any test, the surfaces of the base plate and compression plate were carefully cleaned and inspected to insure they were smooth and free of corrosion. This could reduce the friction between the stainless steel plates and ensure the accuracy of the measurements.

Two types of specimens were used for the experiments (Figure 2): (A) a cylindrical disc with 13mm in diameter and 4mm in thickness and (B) a flat washer with a 5.8 mm I.D., 13 mm O.D. and 4 mm in thickness. All specimens were die cut using ASTM slabs.

The specimens were initially compressed by 25% of their thickness, unless otherwise noted, and the sealing forces were measured. In the thermal cycling test, the temperature varied from $-40\text{ }^{\circ}\text{C}$ to $150\text{ }^{\circ}\text{C}$. A typical temperature profile is seen in Figure 3, as recorded in an experiment. The calculated increase in strain due to thermal expansion between room temperature ($20\text{ }^{\circ}\text{C}$) and $150\text{ }^{\circ}\text{C}$ was approximately 1.9%.

3. Experimental Results

Figures 4 and 5 show the stress relaxation results for both button and washer specimens tested at $20\text{ }^{\circ}\text{C}$ for a period of 24 hrs. The tests were performed at different strain levels: 10%, 25% and 30%. By normalizing the sealing force with the initial force applied, it is observed that the force retention at different strains follow the same magnitude (Figure 6).

Figure 7 shows the stress relaxation results at cycling heating and cooling conditions. It is seen that the sealing forces increase as the temperature increases and decrease as the temperature decreases. This change is due to the thermal expansion of rubber materials. Rubber has a higher coefficient of expansion than the metal flanges. The extent of their difference accounts for an

increase in sealing force at high temperature and a decrease in sealing force at low temperature.

The sealing force measured at cycling heating and cooling conditions provides information on the compound's ability to maintain a seal at conditions to which an actual part may be exposed. The material tested displays good force retention at high temperature (above 120%). The overall force retention after heating and cooling cycles is above 60%.

4. Finite element analysis of stress relaxation

A representative finite element model of continuous compression stress relaxation is shown in Figure 8. The rubber specimen was compressed between a metal plate (bottom) and a rigid surface (top). A reference node was used to control the movement of the rigid surface, and to monitor the load. The friction between rubber block and plates was assumed as 0.01.

Rubber materials display a stress relaxation phenomenon due to their viscoelastic characteristics. The time-domain viscoelasticity of rubber material is modeled with Prony method using ABAQUS (HKS 1998). In Prony series, it assumes a dimensionless relaxation modulus (g_R), which is independent upon the magnitude and direction of straining

$$g_R(t) = \frac{E(t)}{E_0} \quad [1]$$

where E_0 is the instantaneous modulus and $E(t)$ is the relaxation modulus.

In ABAQUS, this dimensionless relaxation modulus (g_R) is incorporated into the elastic constitutive material models. For example, the Ogden's strain energy function:

$$U = \sum_{k=1}^N \frac{2\mu_k}{\alpha_k^2} (\lambda_1^{\alpha_k} + \lambda_2^{\alpha_k} + \lambda_3^{\alpha_k} - 3) + \sum_{k=1}^N \frac{1}{D_k} (J_d - 1)^{2k} \quad [2] \quad \checkmark$$

where the coefficients $\mu_k(\tau)$, and $D_k(\tau)$ are defined by

$$\mu_k(\tau) = \mu_k^0 \left(1 - \sum_{i=1}^n g_i^p (1 - e^{-\tau/\tau_i}) \right)$$

$$\frac{1}{D_k(\tau)} = \frac{1}{D_k^0} \left(1 - \sum_{i=1}^n k_i^p (1 - e^{-\tau/\tau_i}) \right)$$

where

μ_k^0 , and D_k^0 ----- instantaneous shear and bulk behaviors, which define the instantaneous elastic properties.

g_k^p , and k_R^p ----- dimensionless shear and bulk relaxation moduli, which define the viscoelastic properties

To model the stress relaxation of rubber materials, both elastic and viscoelastic properties are required. In the current study, these two properties are defined using experimental data. The instantaneous elasticity is defined by the uniaxial compression data. The viscoelastic property is defined by the normalized stress relaxation data (as shown earlier in Figure 6). The proper choice of the elastic constitutive models can be critical in modeling rubber's viscoelastic behavior. Figure 9 shows the predictions of Ogden and Arruda-Boyce models. It can be seen that these two models give accurate fits to the experimental data.

Figure 10 shows the calculated stress relaxation curves for both button and washer specimens at 20 °C. It is observed that the FEA calculations are in good agreement with the experimental results.

As cycling temperatures are involved, the effect of temperature on material behavior is introduced through the WLF shift function $\log(A)$

$$\log(A) = -C_1(\theta - \theta_0)/(C_2 + \theta - \theta_0) \quad [3]$$

where θ_0 is the reference temperature at which relaxation data is given and C_1 and C_2 are material constants (HKS 1998).

Figure 11 is the calculated stress relaxation curves for both button and washer specimens at cycling temperatures. It is seen that the FEA calculations well predict the first two cycles (room temperature and high temperature), but show a discrepancy for the low temperature cycle. One possible explanation may be that the thermal coefficient can not accurately account for the amount of contraction of rubber component at very low temperature.

5. Conclusions

A new continuous compression stress relaxation tester has been introduced for measuring the sealing force of rubber material under cycling thermal conditions. Compared to the conventional short-term test, the continuous compression stress relaxation provides an improved method for evaluating the suitability of a rubber compound for sealing applications.

Continuous compression stress relaxation at constant temperature has been successfully modeled with finite element method using Prony series. The constitutive material models have been found to have significant effect on the rubber viscoelasticity. The force retention at cycling temperatures were also modeled, although some discrepancy at low temperature was found.

References

Zhang, Y. and Birley, A.W., "A review of the relaxation properties of rubbers", Prog. Rubb. Plast. Technol. 8. Pp318-338, 1992.

Bunting, W.M., Russell, W.D., Doin, J.E., Tate, A.L. and Stocum, G.H., "Compression stress relaxation I: an important test for evaluation of elastomeric materials", SAE paper, No.920135, 1992.

HKS, "ABAQUS user's manual, version 5.8", Hibbit, Karlson and Sorenson, Inc., Pawtucket, RI, 1998

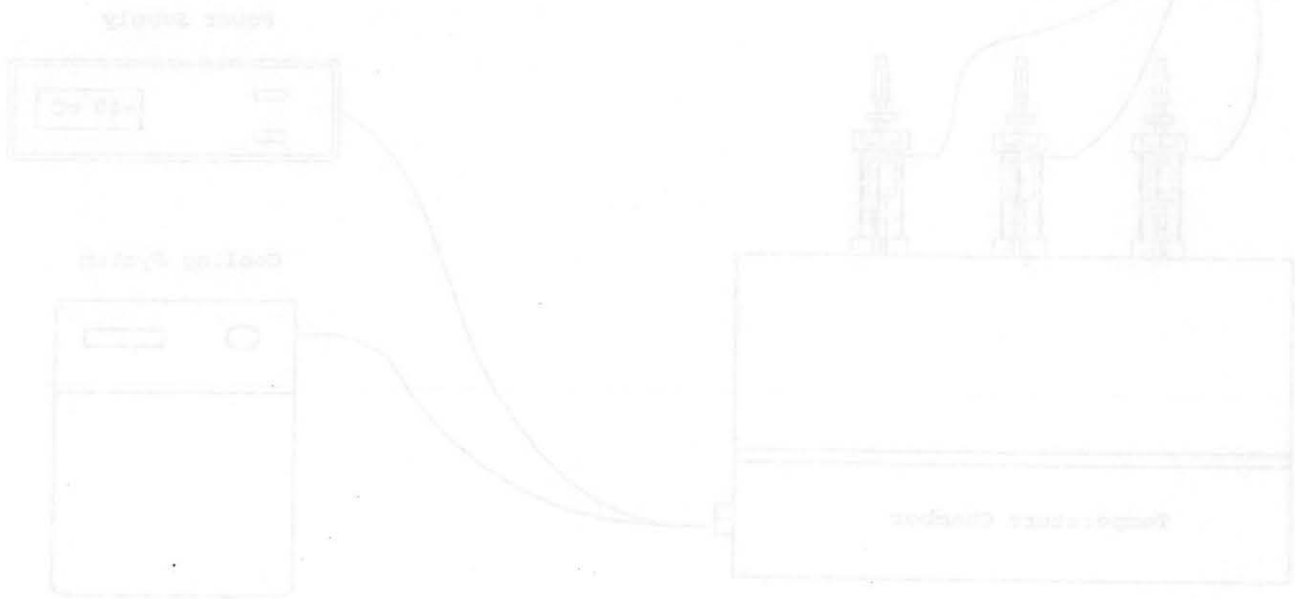


Figure 1a: Schematic of the ARDL continuous compression stress relaxation system.

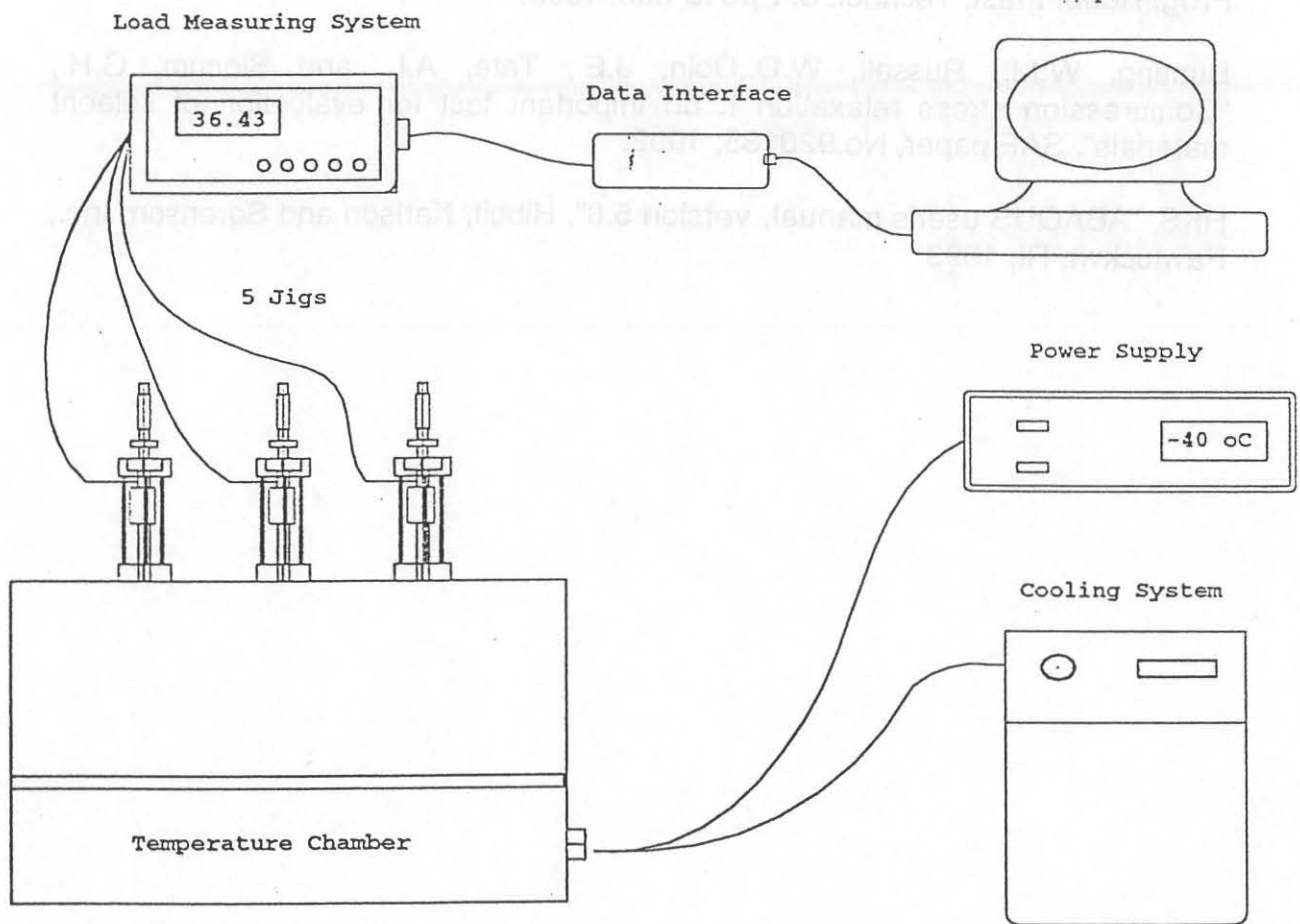


Figure 1a: Schematic of the ARDL continuous compression stress relaxation system.

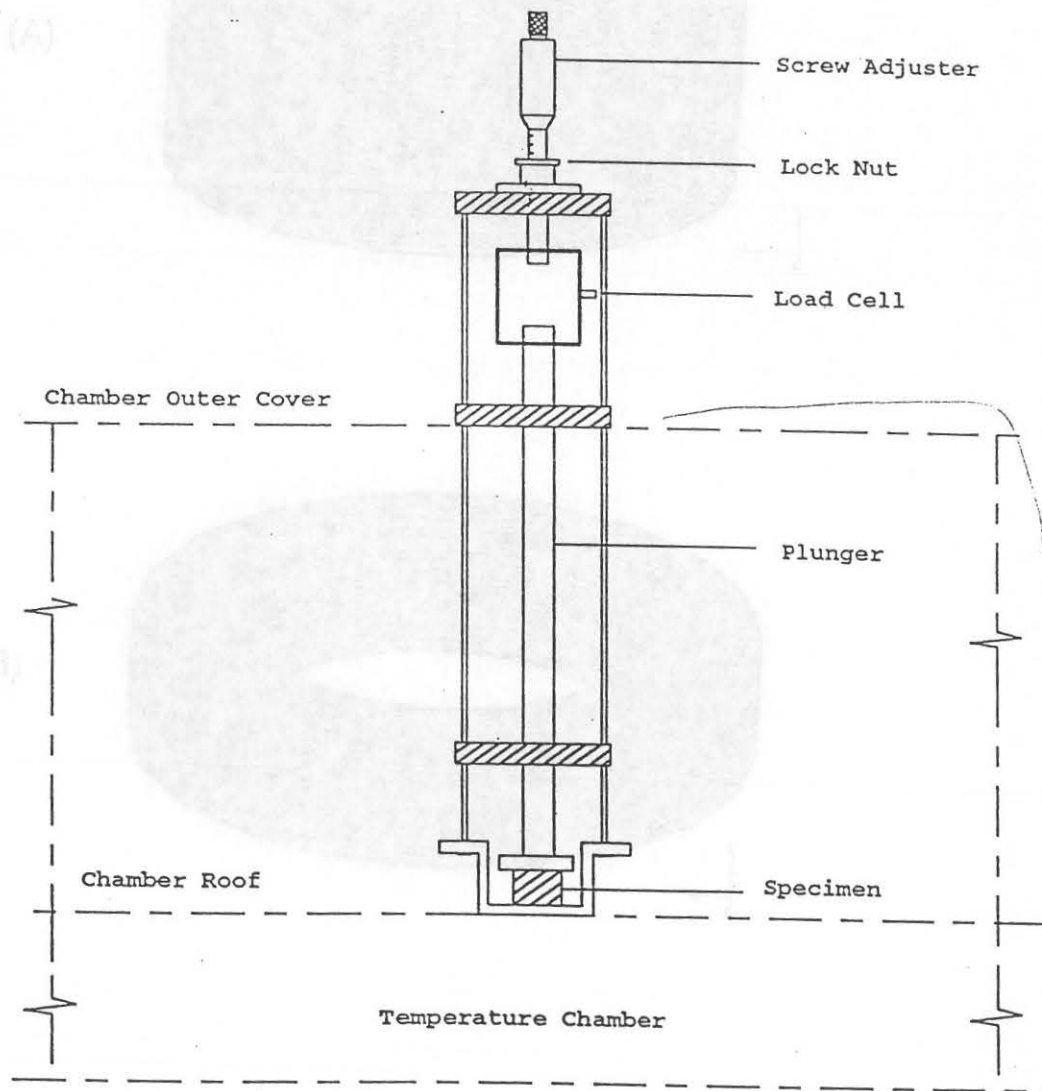


Figure 1b: Detailed drawing of a compression jig.

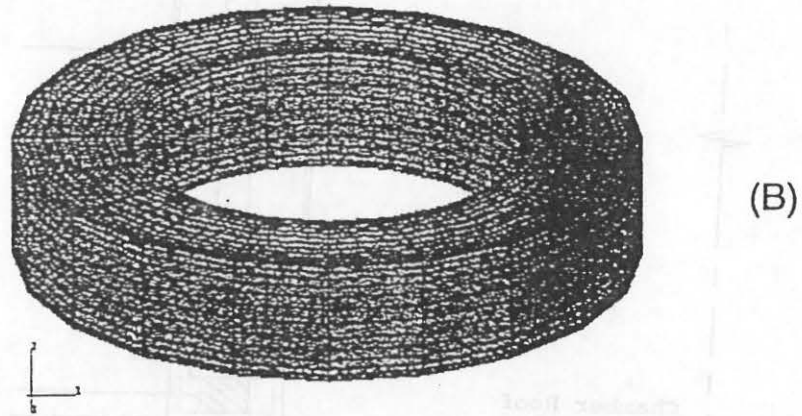
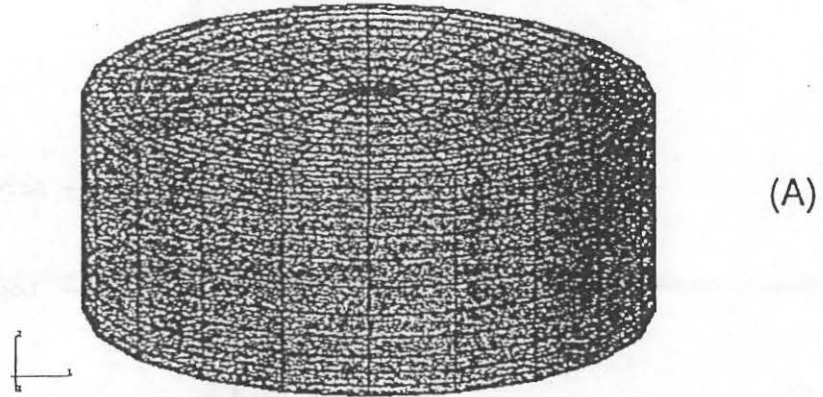


Figure 2: Specimens used for the continuous compression stress relaxation tests: (A) a button and (B) a washer.

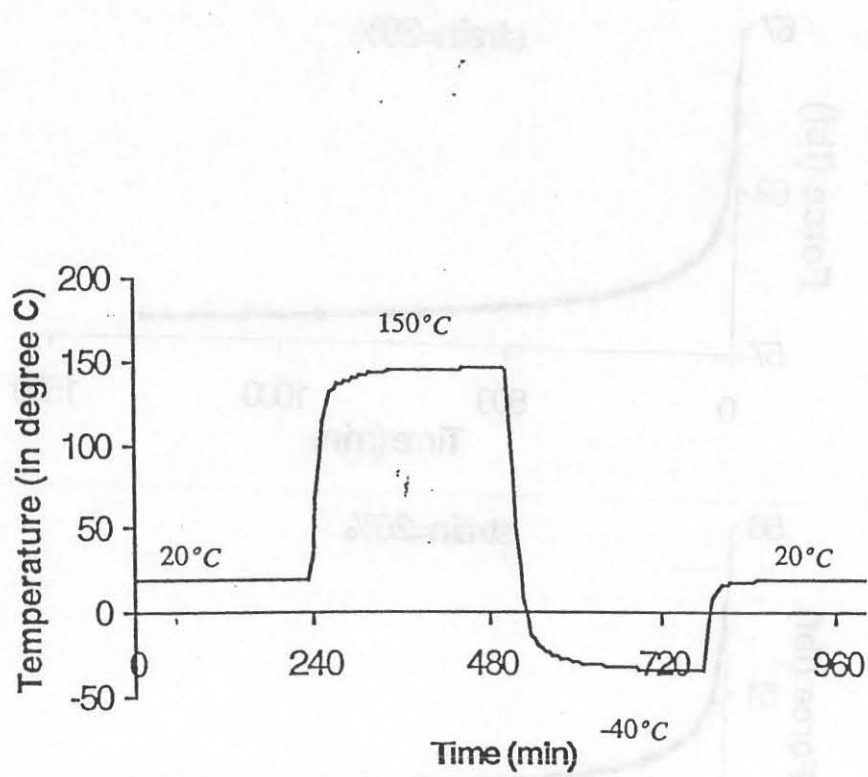


Figure 3: A typical temperature profile as recorded in a thermal cycling test.

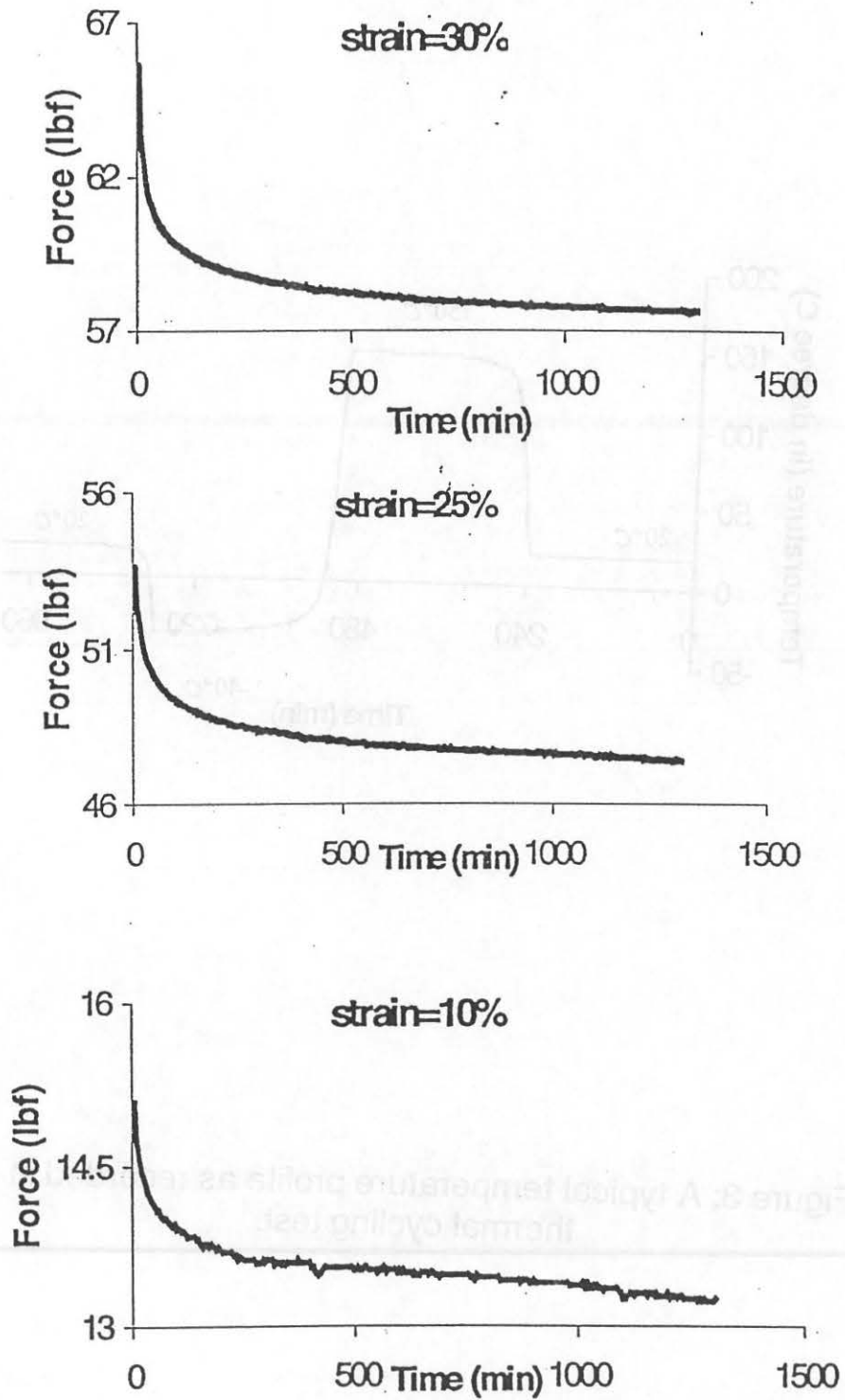


Figure 4: Stress relaxation at 20 °C : button specimen

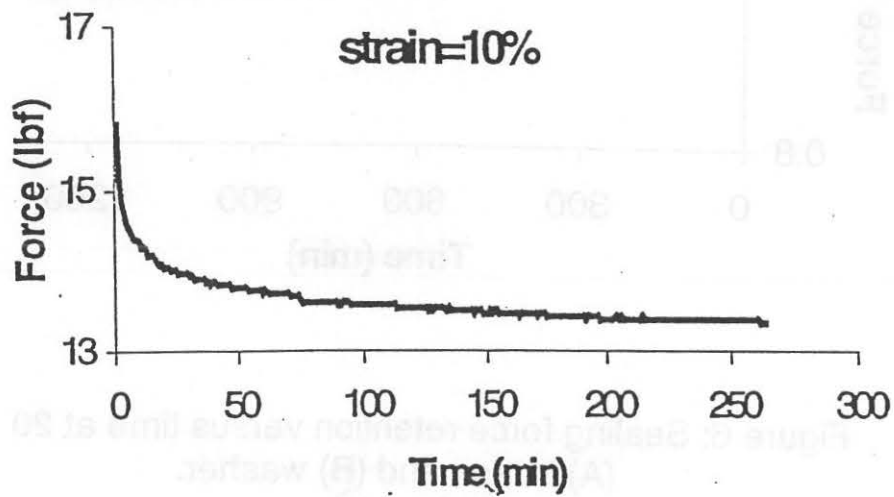
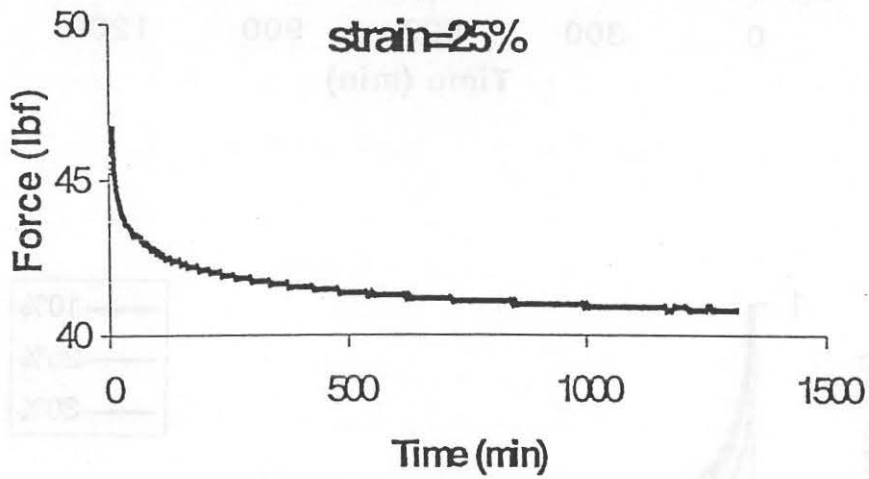
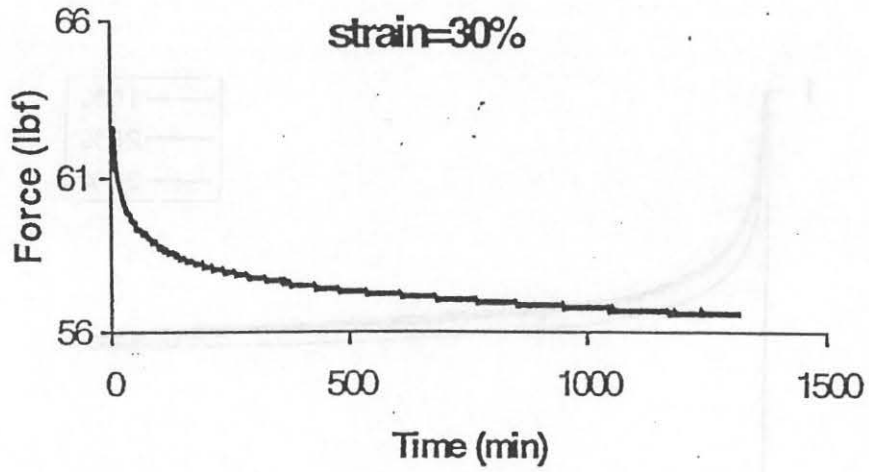
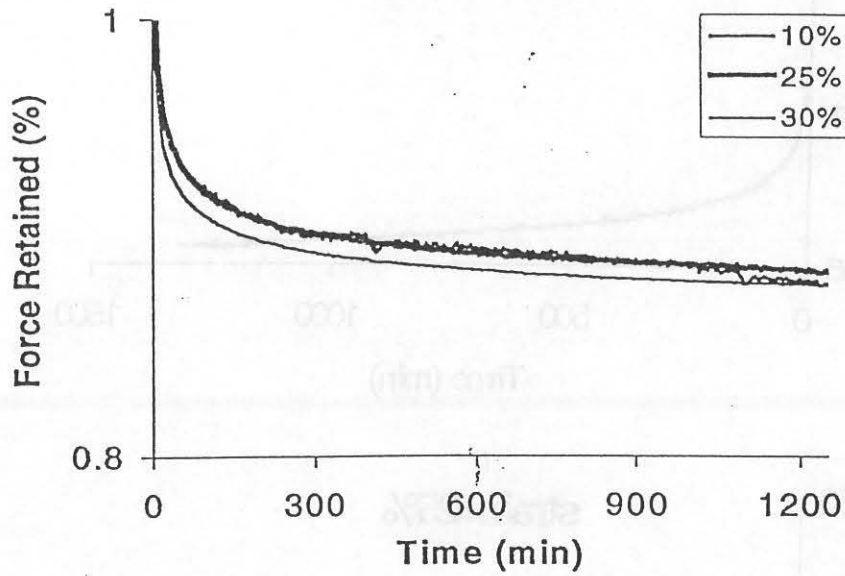
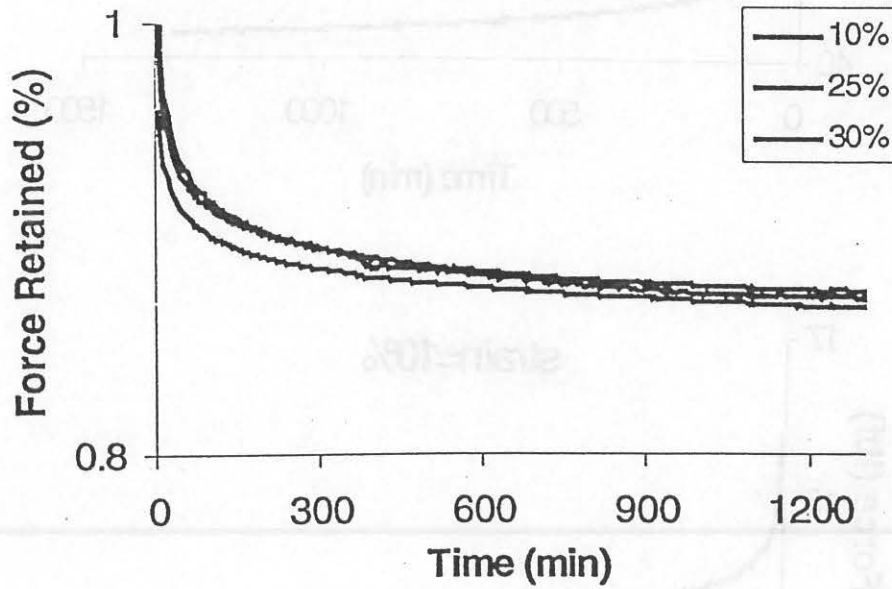


Figure 5: Stress relaxation at 20 °C : washer specimen



(A)



(B)

Figure 6: Sealing force retention versus time at 20 °C :
 (A) button and (B) washer.

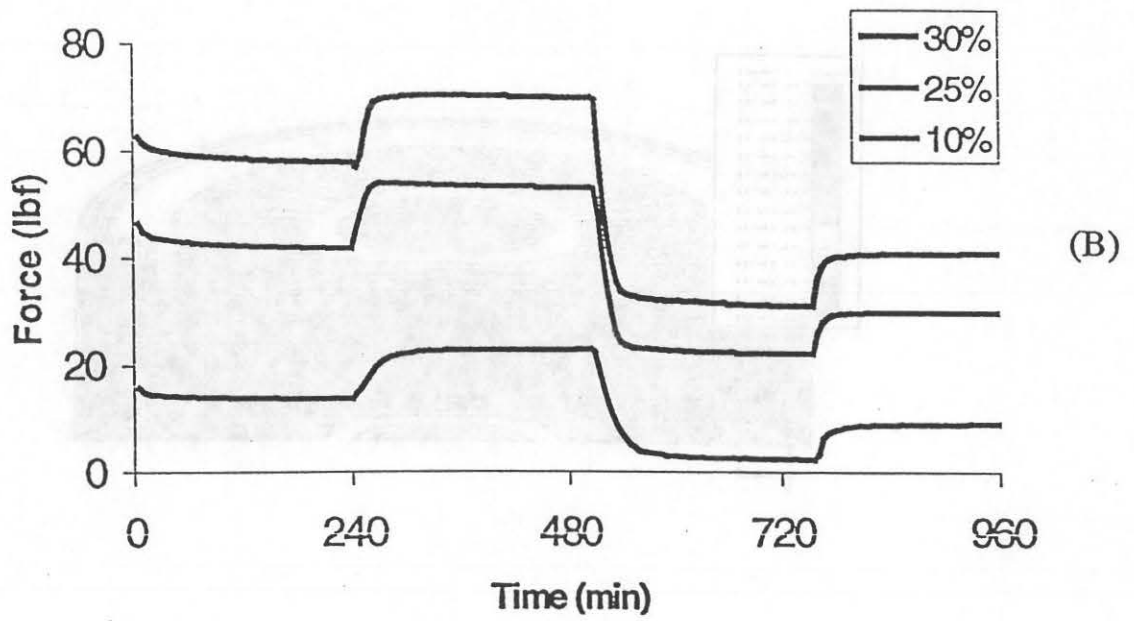
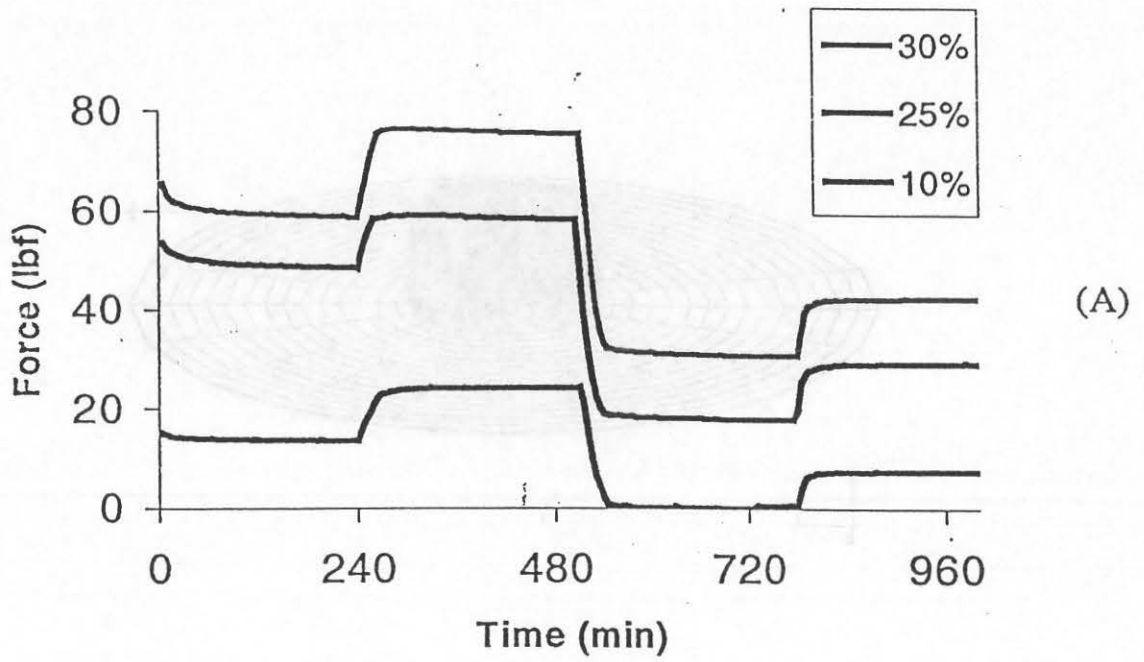


Figure 7: Stress relaxation at cycling heating and cooling: (A) button and (B) washer.

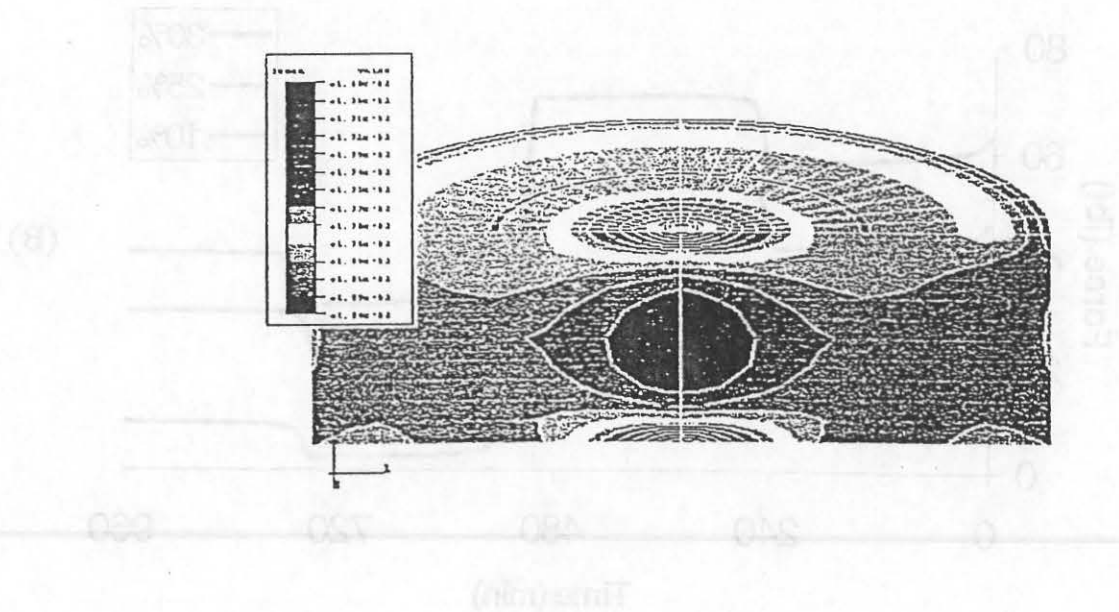
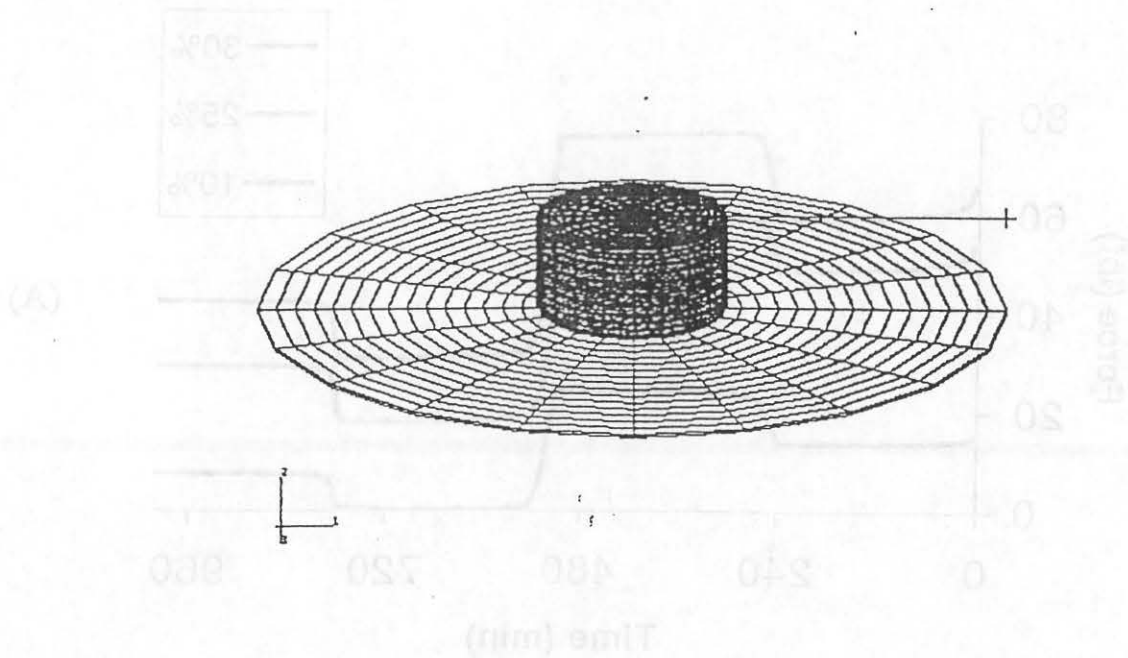


Figure 8: (Above) a button specimen compressed between a metal plate and a rigid surface was used for modeling the CCSR of rubber component; (below) strain energy density contour of a button specimen under compression.

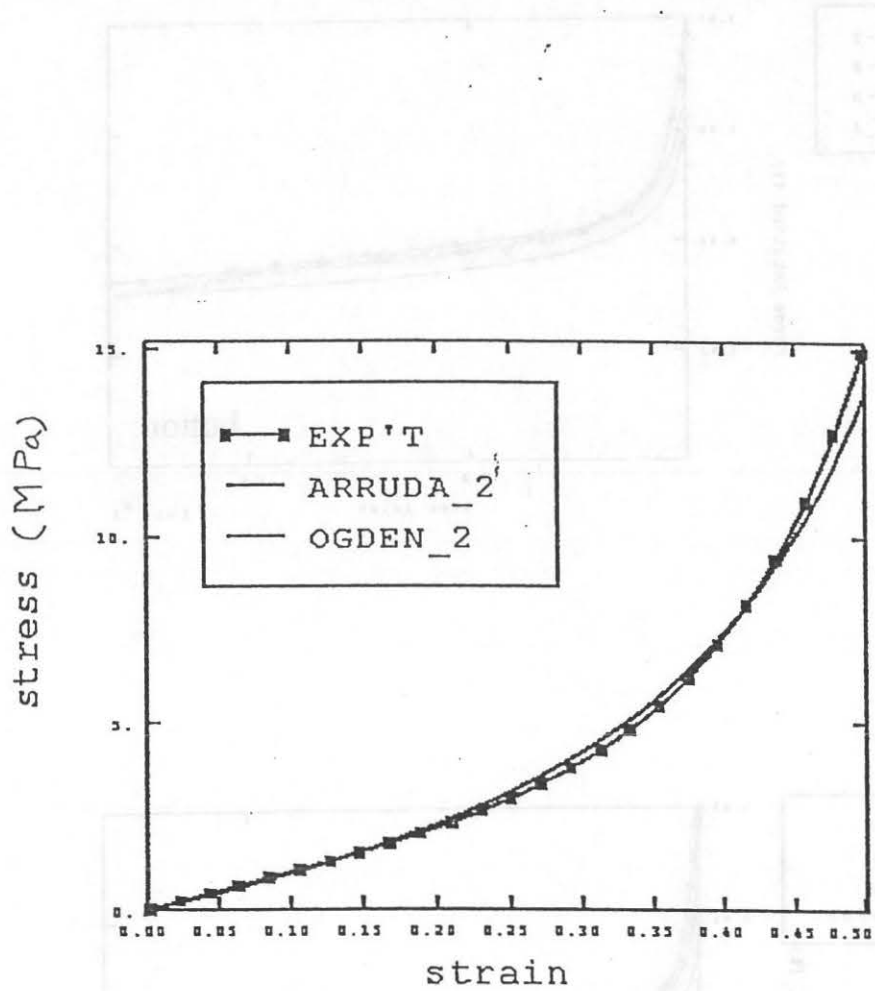


Figure 9: Defining the elasticity of rubber material using constitutive material models

Figure 10: Comparison of CRR at constant temperature (20 °C) experimental vs finite element analysis

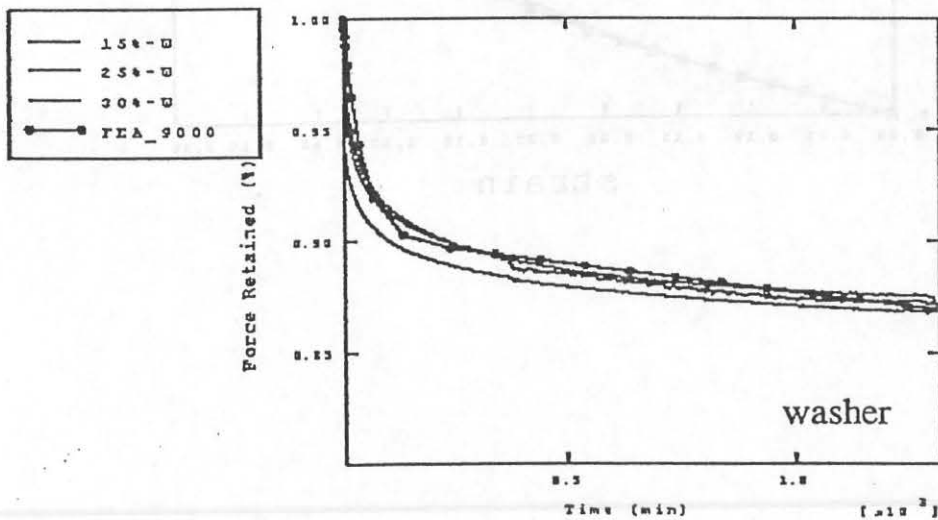
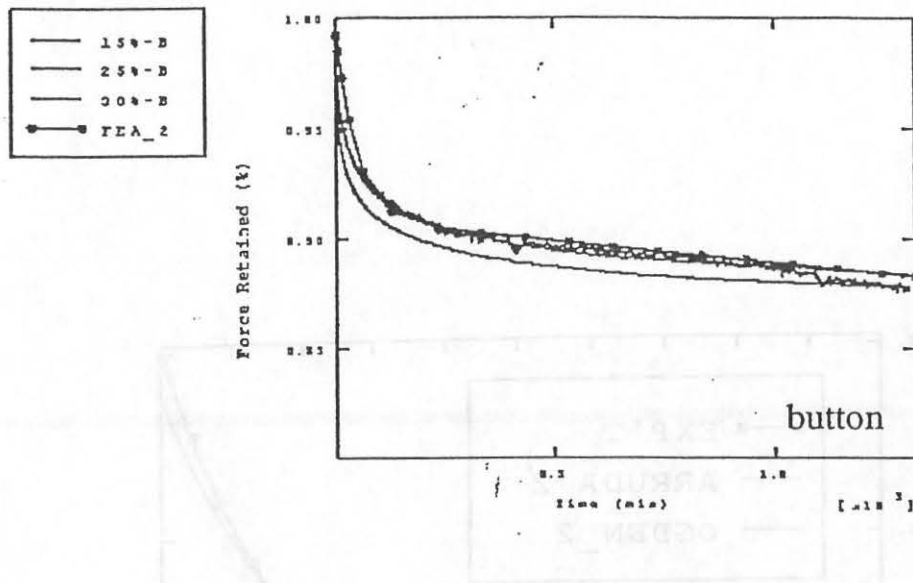


Figure 10: Comparison of CCSR at constant temperature (20 °C): experimental vs. finite element analysis

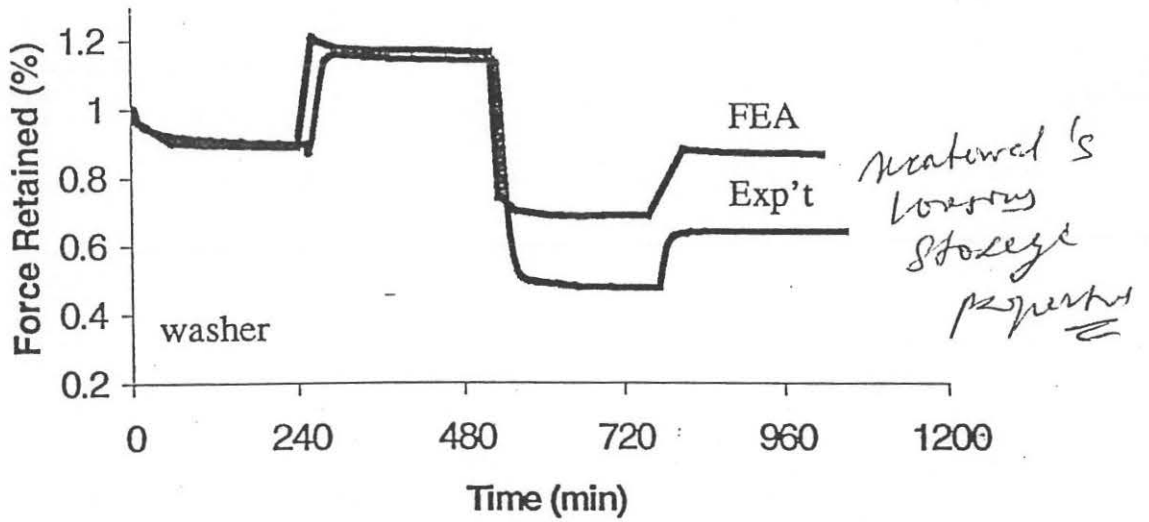
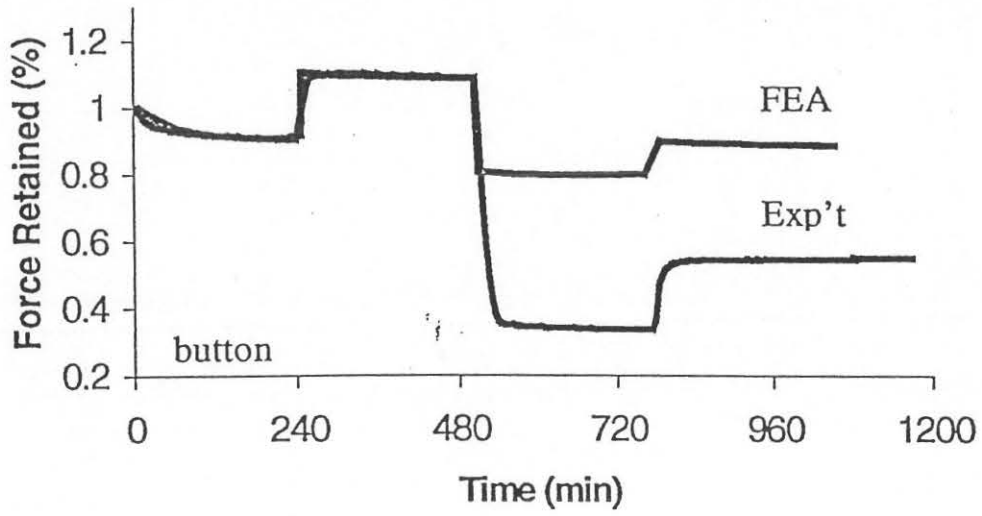


Figure 11: Comparison of CCSR at cycling temperatures: experimental vs. finite element analysis